Polymer 41 (2000) 5865–5870

polymer

Mechanics of rubber particle cavitation in toughened polyvinylchloride (PVC)

E. Crawford, A.J. Lesser*

Polymer Science and Engineering Department, University of Massachusetts, Amherst, MA 01003, USA

Received 28 June 1999; received in revised form 14 October 1999; accepted 18 October 1999

Abstract

The toughening mechanisms and their sequence in rubber modified plastics is determined experimentally through the use of a multi-axial testing combined with and a rubber-modified material with favorable properties. The multi-axial testing was achieved by internally pressurizing and uniaxially loading hollow cylinders. This test allows independent control of the mean stress (volume change) and octahedral shear stress (shape change) between regions of uniaxial compression and equal biaxial tension. The rubber-modified material consists of a methacrylate–butadiene–styrene (MBS) core-shell modifier dispersed in polyvinylchloride (PVC). The whitening behavior of this material during deformation is favorable, since it provides optical verification of cavitation or debonding. In situ light transmission measurements of the MBS modified PVC in the multi-axial stress state test allows the mechanics associated with rubber particle cavitation to be evaluated. The onset of whitening in these systems occurs at a constant octahedral shear stress under a positive mean stress prior to yielding. This behavior is in disagreement with recent models, which predict cavitation occurring at a constant positive mean stress in MBS modified PVC.

Keywords: Rubber toughening; Rubber modification; Particle cavitation

1. Introduction

The addition of rubbery inclusions into a polymeric material is commonly employed to increase the toughness of polymeric materials [1]. Despite the frequent use, the mechanisms and sequence of mechanisms of this toughening are in debate. One opinion is that rubber particle cavitation occurs first to alleviate hydrostatic tension and promote a stress state favorable to shear yielding or shear band formation [2–4]. Another opinion is that rubber particle cavitation occurs after shear band formation [5,6]. Experimental studies investigating these issues are complicated by many factors. For instance, some studies draw conclusions based on post-mortem analyses of fracture surfaces [2,7]. Such analyses reveal the presence of shear bands and cavitated rubber particles yet cannot effectively elucidate the sequence of mechanisms. Studies addressing the sequence of mechanisms often analyze the stress field ahead of a notch [8–10]. The assumptions of the stress field, the positional variation of the stress field, and the amount of constraint in the specimen limit the effectiveness of this approach. A clear experimental approach evaluating the mechanisms and sequence of mechanisms is needed.

Before describing the experimental approach, a brief review of the current thoughts on rubber particle cavitation and yielding in rubber toughened plastics is essential. Rubber particle cavitation, to alleviate hydrostatic tension, is often described from an energy balance approach [3,11,12]. This approach, ignoring some finer details, results in a surface energy term and a strain energy term as shown in Eq. (1).

$$E \approx \Gamma R^2 - K\Delta^2 R^3 \quad (1)$$

where E is the total energy, Γ the surface energy, R the rubber particle size, K the bulk modulus and Δ the volume strain. Two important relationships arise from this energy balance. First, it is more favorable for larger particle to cavitate than smaller particles. Secondly, there is a critical volume strain associated with cavitation of a rubber particle. For an isotropic elastic material, the critical volume strain is linearly related to a critical hydrostatic or mean stress (σ_m) through the bulk modulus. The shaded area in Fig. 1 represents a hypothetical condition for rubber particle cavitation, with a narrow range of particle sizes, in a modified material. An alternative opinion to this criterion describes rubber

* Corresponding author. Tel.: +1-413-577-1316; fax: +1-413-545-0082.
E-mail address: ajl@polysci.umass.edu (A.J. Lesser).

0032-3861/00/$ - see front matter
PII: S0032-3861(99)00787-9

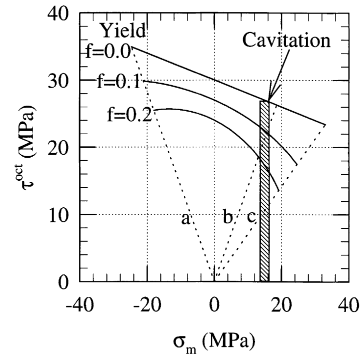

Fig. 1. Yield behavior of cavitated polymeric systems at various void volume fractions. Boxed area represents prediction of rubber particle cavitation from energy balance theories. Dashed lines represent various loading conditions: (a) uniaxial compression; (b) uniaxial tension; and (c) equal biaxial tension.

particle cavitation initiating at the elastic/plastic boundary where plastic flow causes immediate debonding [5,6].

The yield behavior or the elastic/plastic boundary of an isotropic homogenous polymeric material can be characterized by a modified von Mises criterion. For a given state of stress and selecting the octahedral plane, the resulting stress vector can be resolved into two components. The normal component on the octahedral plane is equal to the mean stress, which causes volume change. The parallel component on the octahedral plane is equal to the octahedral shear stress (τ^{oct}), which causes shape change. The critical octahedral shear strength ($\tau_{\text{y}}^{\text{oct}}$) required for yield in a homogenous isotropic polymer has been found to be linearly dependent on the mean stress through the coefficient of internal friction (μ) as described by Eq. (2).

$$\tau_{\text{y}}^{\text{oct}} = \tau_{\text{yo}}^{\text{oct}} - \mu\sigma_{\text{m}} \tag{2}$$

where $\tau_{\text{yo}}^{\text{oct}}$ is the octahedral shear yield strength in absence of a mean stress. The solid line in Fig. 1 with f = 0.0 (void volume fraction) represents this yield criterion.

Recently, researchers [3,13] have proposed various yield loci for porous materials or cavitated polymeric systems based on a model by Gurson [14]. According to one of these criteria, proposed by Bucknall and Lazzeri [3], the introduction of voids (cavitated particles) results in a decrease in yield strength with the amount of decrease dependent on σ_{m}.

$$\left(\frac{\tau_{\text{y}}^{\text{oct}}}{\tau_{\text{yo}}^{\text{oct}}}\right) + \mu\frac{\sigma_{\text{m}}}{\tau_{\text{yo}}^{\text{oct}}}\left(2 - \mu\frac{\sigma_{\text{m}}}{\tau_{\text{yo}}^{\text{oct}}}\right) + 2f\cosh\left(\frac{3\sigma_{\text{m}}}{2\tau_{\text{yo}}^{\text{oct}}}\right) - f^2 - 1 = 0 \tag{3}$$

This behavior is described by Eq. (3) and is represented by the solid lines for various void volume fractions (f) shown in Fig. 1.

Effective evaluation of rubber particle cavitation and yielding in rubber toughened plastics demands materials with favorable properties and unique mechanical tests. The material in this study consists of a methacrylate–butadiene–styrene (MBS) core-shell modifier dispersed in polyvinylchloride (PVC). The material is initially clear but whitens during deformation as shown in Fig. 2. The whitening in MBS modified PVC is attributed to rubber particle cavitation [9,12,15]. This material has favorable properties for studying rubber toughening, since it provides optical verification of rubber particle cavitation. The mechanical test in this study consists of a pressurized and loaded hollow cylinder [16–18]. This test allows a range of stress states, from uniaxial compression to equal biaxial tension (see Fig. 1), to be interrogated with a single specimen geometry. Between the regions of uniaxial compression and equal biaxial tension, the mean stress and the octahedral shear stress can be controlled independently. This stress state control coupled with in situ light transmission measurements of the MBS modified PVC permits evaluation of the mechanisms and sequence of mechanisms in rubber toughened plastics.

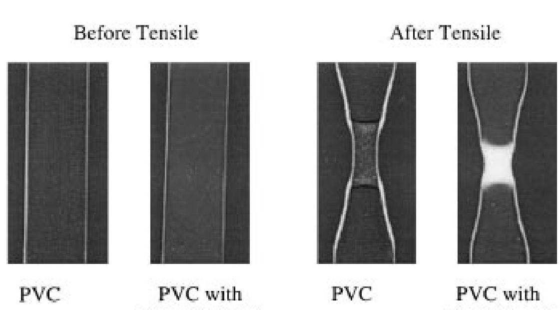

Fig. 2. Contact prints showing the stress whitening behavior of MBS modified PVC with deformation.

2. Experimental

2.1. Material fabrication

The material formulations used in this study consist of the following components:

Component	Product Name	Manufacturer
PVC (K = 58)	Geon 334	The Geon Company
MBS modifier	Paraloid BTA 733	Rohm and Haas
Processing aid	Paraloid K120ND	Rohm and Haas
Heat Stabilizer	Advastab TM-181	Morton International, Inc.
Lubricant	Myverol 18-06	Quest International

The four material formulations were prepared by weight percentage for the various components as shown in Table 1. The formulations were dry blended and compounded by roll-milling at 180°C for 10 min. The resulting sheets,

Table 1
MBS modified PVC formulations showing wt% of each component added

MBS	PVC	Lubricant	Heat stabilizer	Processing aid
0	96	2	2	0
5	90	2	2	1
10	85	2	2	1
15	80	2	2	1

approximately 0.2 mm thick, were then cut for compression molding of sheets and hollow cylinders.

The compression molding of 3 mm thick sheets was performed at 180°C for 10 min. The resulting sheet was machined into tensile specimens (ASTM D638 Type 1) using a specially designed router. The compression molding of hollow cylinders was achieved by a displacement mold [19]. The mold, lightly coated with a silicone mold release, was heated to 190°C in an oven. Fifteen grams of a compounded formulation was placed and compressed into the mold. The mold was left under compression and allowed to cool to room temperature. After cooling, the hollow cylinder was removed from the mold and cut into two 75 mm long specimens. These specimens were then machined with a lathe to create a thin section as shown in Fig. 3. This process ensures whitening will initiate in the area in which light transmission measurements will be made since the stress will be locally higher due to the reduction in cross-sectional area. Gripping of the hollow cylinder was achieved through the use of 15 mm Swagelok® compression fittings and metal inserts as shown in Fig. 3.

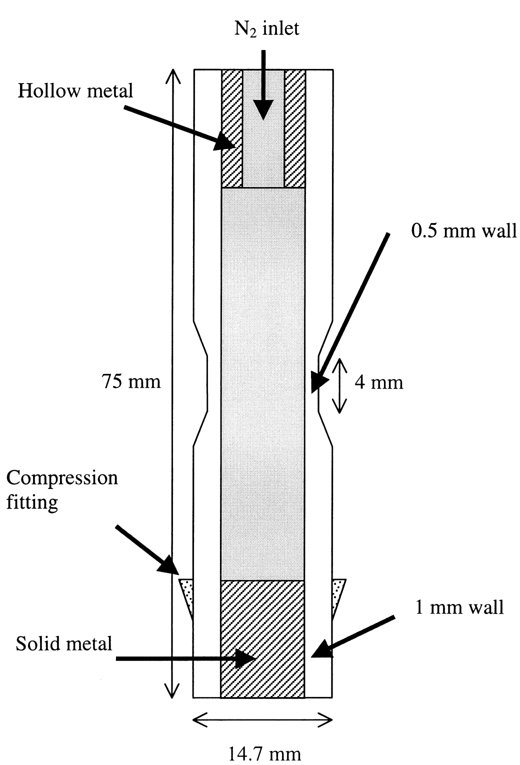

Fig. 3. Hollow cylinder specimen showing thin section.

2.2. Tensile tests

Tensile tests were performed at room temperature and a crosshead speed of 5 mm/min with a Model 1123 Instron equipped with an axial strain gauge to measure the axial extension upon loading and a transverse strain gauge to measure the lateral contraction. Linear regressions were performed on the responses from 0 to 30% of the maximum load to obtain Young's modulus and Poisson's ratio.

2.3. Pressurized and loaded hollow cylinder tests

Hollow cylinder tests were performed at room temperature with a Model 1321 Instron in combination with a Tescom ER3000 pressure regulator controlling the nitrogen pressure. The details of the experimental setup have been described by Kody and Lesser [17]. The stress state in the hollow cylinder, described by Eqs. (4) and (5), is determined by the axial load and the internal pressure in the thin cylinder section.

$$\sigma_1 = \left(\frac{L}{\pi D t}\right) + \left(\frac{PD}{4t}\right) \tag{4}$$

$$\sigma_2 = \left(\frac{PD}{2t}\right) \tag{5}$$

where σ_1 is the axial stress, σ_2 the hoop stress, L the axial load, P the internal pressure, D the mean cylinder diameter and t the thickness. In plane stress conditions ($\sigma_3 = 0$), which is achieved when D/t > 10, the octahedral shear stress is described by Eq. (6) while the mean stress is described by Eq. (7).

$$\tau^{\text{oct}} = \frac{\sqrt{2}}{3}\sqrt{\sigma_1^2 - \sigma_1\sigma_2 + \sigma_2^2} \tag{6}$$

$$\sigma_{\text{m}} = \frac{1}{3}(\sigma_1 + \sigma_2) \tag{7}$$

For a homogenous isotropic material, the octahedral shear strain is related to the octahedral shear stress through the shear modulus. The shear modulus for each formulation was calculated from Young's modulus and Poisson's ratio values obtained from tensile tests. The octahedral shear strain rate was held constant at 0.01 min^{-1} for all loading paths and formulations. On a particular loading path, the ratio of the octahedral shear stress to mean stress was held constant during the entire path. For instance, in uniaxial compression $\tau^{\text{oct}}/\sigma_{\text{m}}$ is equal to −1.41, in uniaxial tension $\tau^{\text{oct}}/\sigma_{\text{m}}$ is equal to 1.41, and in equal biaxial tension $\tau^{\text{oct}}/\sigma_{\text{m}}$ is equal to 0.71. These particular loading paths are displayed as dotted lines *a*, *b* and *c* in Fig. 1.

2.4. In situ light transmission measurements

In situ light transmission measurements were made with a laser diode ($\lambda = 633$ nm, beam diameter = 3 mm) and a 100 mm^2 silicon detector. A linear response between the

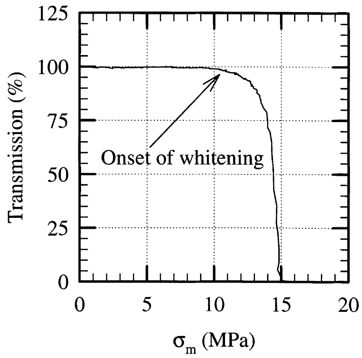

Fig. 4. Light transmission versus mean stress for a uniaxial tension tube test showing the onset of whitening.

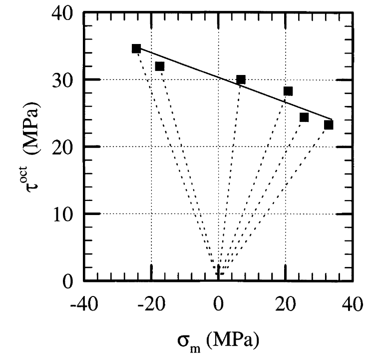

Fig. 5. Yield locus of 0 wt% MBS modified PVC.

measured voltage of the detector circuitry and light intensity was verified through the use of optical density filters. The hollow cylinder specimens were lightly coated with silicon oil to prevent scattering arising from surface roughness. This setup allowed the onset of whitening, signified by a non-linear drop in light transmission to be measured as a function of mechanical deformation to be achieved. Fig. 4 shows a plot of light transmission versus mean stress for a uniaxial tension tube test with the onset of whitening denoted. In situ light transmission measurements were not performed with unmodified PVC, since the materials remain clear during the entire deformational process.

3. Results and discussion

3.1. Elastic properties

The elastic properties for the different formulations are shown in Table 2. With increasing wt% MBS, there is a decrease in Young's modulus (E) and no change in Poisson's ratio (ν). The shear moduli (G) reported in Table 2 and used in the hollow cylinder test to maintain a constant octahedral shear strain rate are calculated using Eq. (8), a formula valid for an isotropic homogenous material.

$$G = \frac{E}{2(1+\nu)} \tag{8}$$

The elastic properties and trends with weight percent MBS modification are consistent with the findings of others [9]. In the rubber modification of many polymeric systems, the gain in toughening outweighs the loss in stiffness and strength [1].

Table 2
Elastic properties of MBS modified PVC at room temperature

Wt% MBS	E (GPa)	ν	G (GPa)
0	3.27	0.38	1.18
5	2.92	0.38	1.06
10	2.47	0.38	0.89
15	2.04	0.38	0.74

3.2. Yield and whitening behavior in multi-axial stress states

The loaded and pressurized hollow cylinder tests coupled with light transmission measurements revealed the yield behavior and whitening behavior of the MBS modified PVC. The unmodified PVC, shown in Fig. 5, shows a modified von Mises yield behavior with $\tau_{yo}^{oct} = 30.1$ MPa and $\mu = 0.18$. This coefficient of internal friction is similar to other polymeric materials [17]. Fig. 6 shows the yield behavior and onset of whitening behavior for 5 wt% MBS modified PVC. The yield behavior again follows a modified von Mises yield behavior with $\tau_{yo}^{oct} = 27.6$ MPa and $\mu = 0.21$. The onset of whitening appears to occur at a relatively constant octahedral shear stress of 15–16 MPa in the positive σ_m half. Whitening did not occur at negative σ_m until yield was reached, resulting in sample buckling and subsequent whitening. The 10 and 15 wt% MBS modified PVC display a similar behavior as shown in Figs. 7 and 8. The yield behavior can be described by a modified von Mises criteria with $\tau_{yo}^{oct} = 26.2$ MPa and $\mu = 0.21$ for the 10 wt% MBS modified PVC and with $\tau_{yo}^{oct} = 24.0$ MPa and $\mu = 0.24$ for the 15 wt% MBS modified PVC. The onset of whitening in the 10 wt% MBS modified PVC occurs at a octahedral shear stress of 14–15 MPa at positive σ_m, while the onset of whitening occurs at 15–16 MPa at positive σ_m half for the 15 wt% MBS modified PVC.

Fig. 9 shows a linear relationship between wt% MBS on

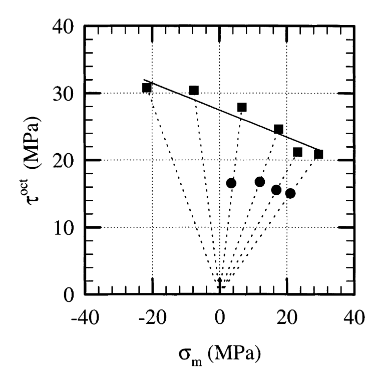

Fig. 6. Yield locus (squares and solid line) and whitening onset (circles) for 5 wt% MBS modified PVC.

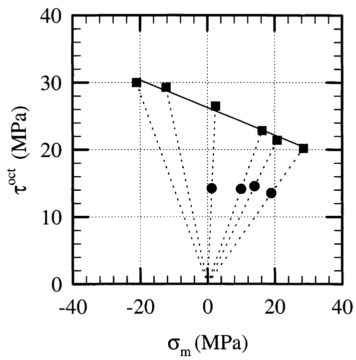

Fig. 7. Yield locus (squares and solid line) and whitening onset (circles) for 10 wt% MBS modified PVC.

the octahedral shear strength in pure shear (τ_{yo}^{oct}). This trend is consistent with Eq. (3), since the incorporation of voids should result in a linear decrease in the τ_{yo}^{oct}.

$$\tau_{yo}^{oct}(f) = \tau_{yo}^{oct}(0)(1 - f) \tag{9}$$

where $\tau_{yo}^{oct}(0)$ is the unmodified octahedral yield strength in pure shear.

It would be difficult to attribute any non-linearity in the yield locus of the modified systems to the inelastic void growth described by Eq. (3). Non-linearity could also arise from slight orientation effects resulting from processing.

The onset of whitening appears to be relatively unaffected by wt% MBS and occurs at a relatively constant octahedral shear stress at positive σ_m. This result is in disagreement with energy balance cavitation theories (Eq. (1)) that describe cavitation (onset of whitening) occurring at a constant positive σ_m. The results indicate that the whitening behavior, which arises from particle cavitation or particle debonding, is a shear-dominated process at positive σ_m.

There are several reports in literature which support these findings. Bensason et al. [9] suggested that the shear yielding precedes particle cavitation at temperatures greater than −20°C in MBS modified PVC. The stress whitening studies by Breuer et al. [15] on MBS modified PVC revealed that ruptured rubber particles occur in bands. These bands of cavitated particles are called dilatational bands and occur in many rubber toughened materials [3]. These bands correspond to shear bands of the matrix material. Since the onset of whitening is shear dominated, it seems likely that cavitation occurs by debonding during shear. Because the onset of whitening appears unaffected by wt% MBS, the data shows the importance of the matrix material's ability to shear. Positive σ_m is only required to open the sheared particle to create a void and scatter light.

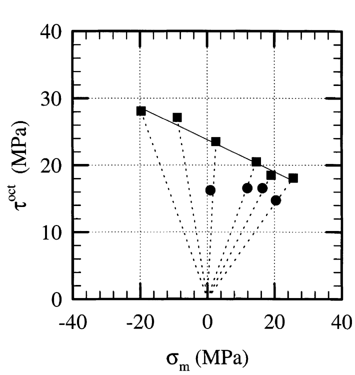

Fig. 8. Yield locus (squares and solid line) and whitening onset (circles) for 15 wt% MBS modified PVC.

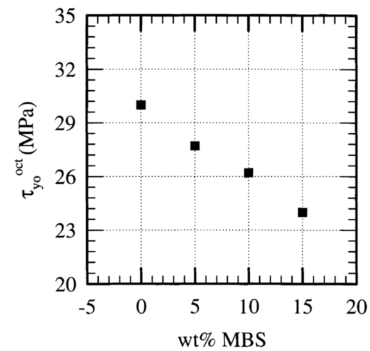

Fig. 9. Octahedral shear strength at $\sigma_m = 0$ as a function of wt% MBS.

Some literature results disagree with the behavior observed in this study. Dompas and Groeninckx [12] used an energy balance approach (constant mean stress criteria) to describe the particle size dependence of the whitening behavior of MBS modified PVC. However, objections can be raised about the experimental procedure used by Dompas and Groeninckx [20] to determine the onset of whitening. Researchers in the field have consistently described the appreciable increase in energy required for fracture arising first from particle cavitation and subsequent shear yielding. The findings of this study do not support this popular opinion. However, the experimental techniques used in this study provide excellent control of the state of stress, allowing separation of shear and volume deformations. In addition, the materials used in this study provide favorable properties for determining cavitation or debonding processes. This combination allows for an effective study of the mechanics of rubber toughened polymeric systems.

Acknowledgements

The authors wish to acknowledge the financial support of Shell Chemical Co. Elastomers Department. The authors would also like to thank Drs Mike Modic and Mike Masse at Shell Chemical Co. for their helpful comments and suggestions.

References

[1] Bucknall CB. In: Haward RN, Young RJ, editors. The physics of glassy polymers, 2. London: Chapman & Hall, 1997. pp. 363 chap. 8.
[2] Yee AF, Pearson RAJ. Mater Sci 1986;21:2462.

[3] Lazzeri A, Bucknall CBJ. Mater Sci 1993;28:6799.
[4] Lu F, Cantwell WJ, Kausch HHJ. Mater Sci 1997;32:3059.
[5] Evans AG, Ahmad ZB, Gilbert DG, Beaumont PW. Acta Metall 1986;34:79.
[6] Dekkers ME, Hobbs SY, Watkins VHJ. Mater Sci 1988;23:1225.
[7] Pearson RA, Yee AFJ. Mater Sci 1989;24:2571.
[8] Parker DS, Sue H-J, Huang J, Yee A. Polymer 1989;31:2267.
[9] Bensason S, Hiltner A, Baer E. J Appl Polym Sci 1997;63:715.
[10] Tse A, Shin E, Hiltner A, Baer E. J Mater Sci 1991;26:5374.
[11] Bucknall CB, Karpodinis A, Chang XC. J Mater Sci 1994;29:3377.
[12] Dompas D, Groeninckx G. Polymer 1994;35:4743.
[13] Steenbrink AC, Giessen VD, Wu E. J Mech Phys Solids 1997;45:405.
[14] Gurson ALJ. J Engng Mater Technol, Trans ASME 1977;99:2.
[15] Breuer H, Haaf F, Stavenow JJ. Macromol Sci Phys 1977;14:387.
[16] Sultan J, McGarry F. J Polym Engng Sci 1972.
[17] Kody RS, Lesser AJJ. Mater Sci 1997;32:5637.
[18] Tuttle ME, Semeliss M, Wong R. Exp Mech 1992;32:1.
[19] Butler J. Compression and transfer molding, New York: Interscience, 1959.
[20] Dompas D, Groeninckx G. Polymer 1994;33:4750.